Modelling transcriptional feedback loops: the role of Gro/TLE1 in Hes1 oscillations

By Samuel Bernard[1], Branka Čajavec[1], Laurent Pujo-Menjouet[2], Michael C. Mackey[3,*] and Hanspeter Herzel[1]

[1]*Institute for Theoretical Biology, Humboldt University, Invalidenstrasse 43, 10115 Berlin, Germany*
[2]*Department of Mathematics, Vanderbilt University, 1326 Stevenson Center, Nashville, TN 37240, USA*
[3]*Departments of Physiology, Physics & Mathematics and Centre for Nonlinear Dynamics, McGill University, 3655 Promenade Sir William Osler, Montreal, Quebec H3G 1Y6, Canada*

The transcriptional repressor Hes1, a basic helix-loop-helix family protein, periodically changes its expression in the presomitic mesoderm. Its periodic pattern of expression is retained in a number of cultured murine cell lines. In this paper, we introduce an extended mathematical model for Hes1 oscillatory expression that includes regulation of Hes1 transcription by Drosophila Groucho (Gro) or its vertebrate counterpart, the transducine-like enhancer of split/Groucho-related gene product 1 (TLE1). Gro/TLE1 is a necessary corepressor required by a number of DNA-binding transcriptional repressors, including Hes1. Models of direct repression via Hes1 typically display an expression overshoot after transcription initiation which is not seen in the experimental data. However, numerical simulation and theoretical predictions of our model show that the cofactor Gro/TLE1 reduces the overshoot and is thus necessary for a rapid and finely tuned response of Hes1 to activation signals. Further, from detailed linear stability and numerical bifurcation analysis and simulations, we conclude that the cooperativity coefficient (h) for Hes1 self-repression should be large (i.e. $h \geq 4$). Finally, we introduce the characteristic turnaround duration, and show that for our model the duration of the repression loop is between 40 and 60 min.

Keywords: Hes-1; Gro/TLE1; Hill coefficient; transcriptional repression loop; turnaround duration

1. Introduction

Recent experiments on cultured mammalian cell lines have shown oscillatory dynamics in the expression of at least three transcriptional factors: Hes1, p53 and NF-κB (Lev Bar-Or *et al.* 2000; Hirata *et al.* 2002; Hoffmann *et al.* 2002). In this paper, we deal with one of them, Hes1. We propose an extended model for the

regulation of Hes1 expression that explains its oscillatory nature, and look for parameter requirements in different versions of the model.

Somites are transient embryonic structures that are formed through segmentation of the presomitic mesoderm (PSM) in a highly regulated process called somitogenesis. They are the origin of the skeletal muscles of the body as well as the axial skeleton and the dermis of the back (Christ & Ordahl 1995). The partitioning of the vertebrate body into a repetitive series of somites requires the spatially and temporally coordinated behaviour of the cells in PSM. This is achieved by an oscillatory mechanism generating periodic waves of gene expression (order of 2 h) known as segmentation clock (Schnell *et al.* 2002).

The genes that are periodically expressed belong to the HES family (for Hairy Enhancer of Split; Gao *et al.* 2001). They act by negatively regulating transcription of tissue-specific transcription factors (Ohsako *et al.* 1994). The transcription factor Hes1 is essential to neurogenesis, myogenesis, haematopoiesis and sex determination (Proush *et al.* 1994; Ishibashi *et al.* 1995). Hirata *et al.* (2002) showed that a single serum treatment induces an oscillation of Hes1 mRNA and protein concentrations with a 2 h period in a variety of cultured cells, such as myoblasts, fibroblasts, neuroblastoma cells and teratocarcinoma. They also showed that Hes1 acts as its own repressor through a negative feedback loop. To account for the appearance of these oscillations, they proposed the involvement of a third factor in addition to Hes1 protein and Hes1 mRNA, because three species are necessary to induce oscillations in a negative feedback system (Griffith 1968). However, the introduction of an explicit delay of 15–20 min in a basic two-species model with negative feedback is also sufficient to explain the oscillations (Jensen *et al.* 2003; Monk 2003). The delay accounts for the time needed for transcription, translation and formation of a complex in the nucleus to start repression.

Drosophila Groucho (Gro) and its vertebrate counterparts, the transducine-like enhancer of split/Groucho-related gene products 1–4 (TLEs1–4), lack DNA binding ability but can functionally associate with a number of DNA-binding proteins, including Hes1. Interaction with Gro/TLE1 at the nuclear matrix is necessary for transcriptional repression by Hes1 (McLarren *et al.* 2001). Hes1 itself activates hyperphosphorylation of Gro/TLEs bound to it. This correlates with association of Gro/TLE1 to a nuclear matrix, suggesting that chromatin remodelling might be a mechanism for this transcriptional repression (Nuthall *et al.* 2002). We present here a model that includes Gro/TLE1 in the regulation of Hes1-mediated repression of transcription.

Ordinary differential equations (ODEs) with negative feedback loops need to be at least three-dimensional to sustain oscillations. A requirement for these oscillations is a high cooperativity coefficient, i.e. a large feedback gain is necessary for the onset of oscillations (Tyson & Othmer 1978). One such system, the Goodwin model (Goodwin 1965), has been extensively used in circadian clock modelling. However, this model requires a cooperativity coefficient of at least 9 to induce oscillations, which is large and unrealistic unless a cascade mechanism is involved (Ferrell 1996). On the other hand, the introduction of a time delay in a feedback loop allows sustained oscillations even in a one-dimensional delay differential equation with a relatively low cooperativity coefficient.

Time-series of Hes1 mRNA and protein levels in various cell cultures were used as a starting point for modelling Hes1 repression loop. This paper considers

two different models of self-repression kinetics, and uncovers conserved features among them. Section 2 presents an analysis of the two-dimensional system proposed by Jensen *et al.* (2003). In §3, we develop an extension of the Jensen *et al.* model considering Gro/TLE1 interaction with the Hes1 regulatory pathway. We then discuss the effects of Gro/TLE1 on the properties of oscillatory Hes1 expression after initiation by a serum shock. Section 4 considers general features of the two models that allow the estimation of parameter values. We find quantities that are relatively invariant with respect to different models. We conclude that although interaction of Hes1 with the corepressor Gro/TLE1 is not necessary for oscillatory expression of Hes1, it does allow a much more realistic activation curve that is consistent with the experimental data.

2. Two-dimensional Hes1–mRNA repression model

Standard mathematical analysis shows that two-component models with a negative feedback cannot have stable self-sustained oscillations. Two possibilities are then offered for a simple extension of the model to achieve oscillatory behaviour.

First, one can invoke the existence of a third dependent variable. This is the route taken by Hirata *et al.* (2002) who have considered a three-dimensional system, in which a third (unknown) species X actively degrades Hes1, while Hes1 also acts as a repressor for X. However, the analysis of this model is not further considered in this paper. Second, an explicit delay (Jensen *et al.* 2003; Monk 2003; Lewis 2003) is considered, which has its origin in the underlying biology. In either case the Hill coefficient h, which accounts for the cooperativity of repression activity of agents involved in the inhibition of Hes1 transcription, is crucial. Although these studies dealt with parameter estimation and stability analysis, the cooperativity coefficient h was taken as a fixed parameter with a value between 2 and 4. The complexity of transcription regulation does not allow for direct evaluation of the cooperativity coefficient, so we analysed a self-repression to find plausible ranges of the value of h.

A two-compartment model for Hes1–mRNA self-repression with delay can be written as (Jensen *et al.* 2003; Monk 2003; Lewis 2003)

$$\frac{\mathrm{d}mRNA(t)}{\mathrm{d}t} = \frac{f_0 k^h}{k^h + Hes1(t-\tau)^h} - \delta mRNA(t), \tag{2.1}$$

$$\frac{\mathrm{d}Hes1(t)}{\mathrm{d}t} = \beta mRNA(t) - \alpha Hes1(t). \tag{2.2}$$

Equations (2.1) and (2.2) will be referred to as Model A. The first equation describes the cellular concentration of Hes1 mRNA ($mRNA$) at time t and the second equation describes the cellular concentration of Hes1 protein ($Hes1$) at time t. The respective degradation rates (δ of $Hes1$ and α of $mRNA$) and translation rate (β) all have units of $\min^{-1}$. The nonlinearity comes from the transcriptional repression activity of Hes1. The parameters in the feedback loop are the maximum mRNA transcription rate f_0 (conc $\min^{-1}$), a DNA dissociation constant k (same units as $Hes1$) and a Hill coefficient h representing the degree of cooperativity between different factors intervening in the repression of *Hes1* gene

Table 1. List of parameters. (Parameters used for simulations and analysis. The letter 'm' indicates that the parameter was estimated from model analysis. References are: 1, Hirata *et al.* (2002); 2, Jensen *et al.* (2003) and Monk (2003); 3, Bolouri & Davidson (2003).)

parameter	value	units	ref.	description
α	0.03	$\min^{-1}$	(1)	Hes1 degradation rate
δ	0.03	$\min^{-1}$	(1)	mRNA degradation rate
σ	0.03	$\min^{-1}$	m	GroH deactivation rate
k, ℓ	—	conc.	(2)	see appendix A
h	2–4	—	(2),m	Hes1 repression cooperativity; lower bound
u	2–4	—	m	GroH activation cooperativity; lower bound
T_{Hopf}	90–150	min	(1)	period of oscillation of Hes1
τ	10–30	min	(2),m	total delay due to transcription, translation and transport; upper bound
f_0	1	conc. $\min^{-1}$	(3)	maximal transcription/translation rate see appendix A
g_0	1	$\min^{-1}$	—	maximal phosphorylation rate
β	1	$\min^{-1}$	(3)	Hes1 translation rate

by Hes1 protein. The delay τ accounts for the delay due to Hes1 modification, complex formation and nucleocytoplasmic molecular transport.

Table 1 gives the values of parameters used for the analysis and simulations. The experimentally measured parameters are the decay rates α and δ, and the period of oscillation T_{Hopf}. The deactivation rate σ was assumed to be of the same order as the degradation rates. We have performed a numerical sensitivity analysis by varying every parameter from 0.1 to 10 times their default value. We looked at the presence of oscillations and the period of oscillation. We found that the oscillations were present for most of the parameter values and that the period changed by less than 15% with respect to f_0, g_0, k, ℓ and β (results not shown). Degradation rates had a marked influence on the behaviour of the system, but they have been measured accurately (Hirata *et al.* 2002). Therefore, the following analysis mainly focuses on the effect of the Hill coefficients h and u and the explicit delay τ. The details of the computations and analysis are given in appendices A–C.

The bifurcation diagram with respect to h (figure 1*a*) indicates the two possible behaviours of Hes1 activity: damping to a steady state or sustained oscillations, with an increasing period (figure 1*c*). Experimental levels of Hes1 mRNA and protein oscillate with a relatively constant amplitude and a 2 h period (figure 1*b*).

In this model, a stability analysis (cf. appendix A) leads to analytical formulae for local stability connecting the Hill coefficient, Hopf (oscillation) period and rate constants. Namely, the steady state is unstable and a limit cycle is obtained whenever h is larger than

$$h_{\text{crit}}^{\text{A}} = \left[\left(\frac{4\pi^2}{\alpha\delta T_{\text{Hopf}}^2} + \frac{\delta}{\alpha} \right) \left(\frac{4\pi^2}{\alpha\delta T_{\text{Hopf}}^2} + \frac{\alpha}{\delta} \right) \right]^{1/2}. \tag{2.3}$$
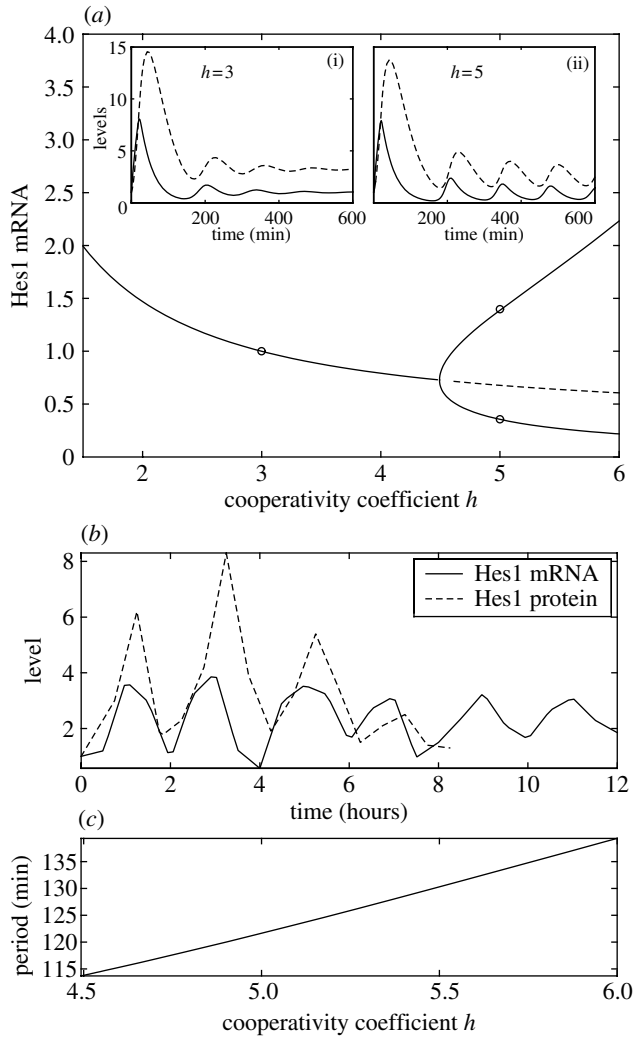
Figure 1. (*a*) Numerically computed bifurcation diagram of Model A as a function of *h*. The main panel shows the stable steady state and limit cycle (solid line) and unstable steady state (dashed line). For *h*=3, mRNA and protein levels converge to a steady state (panel (i)). For *h*=5, the solution converges to a stable limit cycle (panel (ii)). A Hopf bifurcation occurs at *h*=4.5. (*b*) Experimental time-series of Hes1 mRNA and protein levels (Hirata *et al.* 2002). (*c*) Period of oscillation of the limit cycle as a function of *h*. Parameters as in table 1, with τ=18 min.

Note that this critical value of *h* does not depend on the delay τ. Rather, we use the Hopf period T_{Hopf} as a parameter and let τ depend on T_{Hopf}. This allows us to place bounds on *h* and τ. Assuming a period $T_{\text{Hopf}} = 120$ min, we obtain a lower bound on the cooperativity coefficient $h_{\text{crit}}^{\text{A}} \simeq 4.1$. For a given cooperativity coefficient *h* and Hopf period T_{Hopf}, the associated critical delay $\tau_{\text{crit}}^{\text{A}}$ can be expressed as

$$\tau_{\text{crit}}^{\text{A}} = \frac{1}{\omega}\arccos\left(\frac{\omega^2}{\alpha\delta h} - \frac{1}{h}\right), \tag{2.4}$$
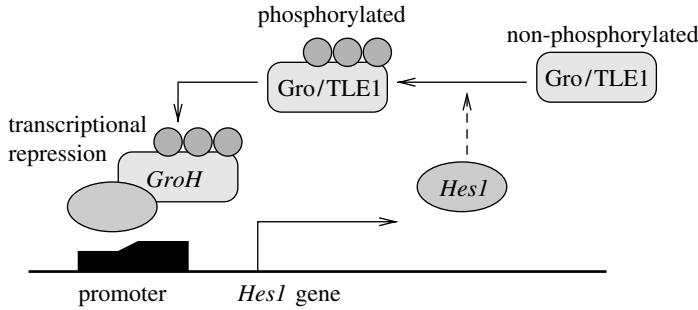
Figure 2. Model for Gro/TLE1-mediated Hes1 repression.

where ω is the oscillatory angular frequency, $\omega = 2\pi/T_{\mathrm{Hopf}}$. The critical delay defines the boundary between stable ($\tau < \tau_{\mathrm{crit}}^{\mathrm{A}}$) and oscillatory ($\tau > \tau_{\mathrm{crit}}^{\mathrm{A}}$) mRNA and protein levels. This leads to a value of the maximal $\tau_{\mathrm{crit}}^{\mathrm{A}}$, $\tau_{\mathrm{A}} \simeq 19.7$ min.

When Model A has no explicit delay ($\tau = 0$), its characteristic time-scale (CTS), defined as $1/|\mathrm{Re}(\lambda)|$ with λ the eigenvalue of Model A, is determined by the decay rates α and δ (Murray 1993; Strogatz 1994). Explicitly, CTS= $2(\alpha + \delta)^{-1} = 33.3$ min. Added to $\tau_{\mathrm{A}} = 19.7$ min, it gives a characteristic turn-around duration (CTD) of $\mathrm{CTD} = \mathrm{CTS} + \tau_{\mathrm{A}} = 53$ min. The turnaround duration is the time required to have an effective repression after transcription initiation (see appendix B for a derivation of these results).

The value τ_{A} constitutes an upper bound on the delay and $h_{\mathrm{crit}}^{\mathrm{A}}$ is a lower bound on the cooperativity coefficient. To have large amplitude oscillations (i.e. to move away from the bifurcation point), it is necessary to have a somewhat smaller τ and/or larger h.

3. Gro/TLE1-mediated repression allows tuned response

(a) Gro/TLE1–Hes1 repression model

We now consider the influence of an additional factor known to be involved in the Hes1 repression loop, namely Gro/TLE1. Protein Gro/TLE1 is activated through Hes1-induced hyper-phosphorylation. This activation is described by a Hill function that is a monotonically increasing function of Hes1 with Hill coefficient u. Moreover, the active form of Gro/TLE1 forms a complex with Hes1, denoted *GroH*, to mediate repression through a negative feedback loop (cf. figure 2). The variable *GroH* represents the repression complex of hyper-phosphorylated Gro/TLE1 with Hes1 protein. The associated equations are written as

$$\frac{\mathrm{d}Hes1(t)}{\mathrm{d}t} = \frac{f_0 k^h}{k^h + GroH(t-\tau)^h} - \alpha Hes1(t), \tag{3.1}$$

$$\frac{\mathrm{d}GroH(t)}{\mathrm{d}t} = \frac{g_0 Hes1(t)^u}{\ell^u + Hes1(t)^u} - \sigma GroH(t). \tag{3.2}$$

These equations constitute what we call Model B. As with the other model, local stability considerations establish relationships between the Hill coefficient,
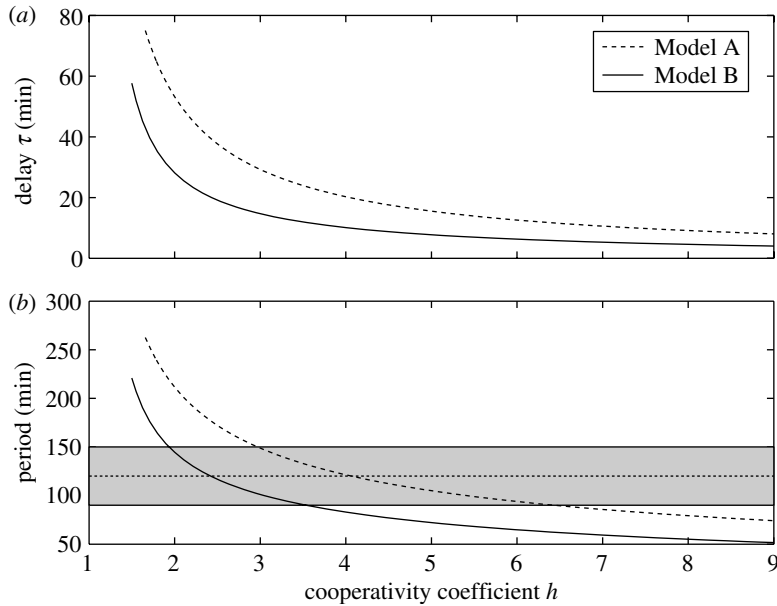
Figure 3. Comparison between numerical bifurcation analysis of Model A (dashed lines) and Model B (solid lines). Note that the small Hill coefficient needed in case of Model B comes from the fact that the total cooperativity coefficient is $h \times u$. (*a*) The bifurcation curves give the delay τ required to induce a Hopf bifurcation for a given h. Crossing the lines from left to right (or from below) due to parameter variation induces oscillations (e.g. figure 1). (*b*) Associated periods for each bifurcation curve are shown. The grey area indicates the period interval from 90 to 150 min, delineating a corresponding range of Hill coefficients.

period, kinetic constants and delay. Following the same analytical development as for Model A, we found that the quantity playing the role of the Hill coefficient was now the product of h and u. Denoting this quantity total cooperativity, $c = uh$, we obtain an expression similar to equation (2.3):

$$c_{\text{crit}} = \left[\left(\frac{4\pi^2}{\alpha\sigma T_{\text{Hopf}}^2} + \frac{\sigma}{\alpha} \right) \left(\frac{4\pi^2}{\alpha\sigma T_{\text{Hopf}}^2} + \frac{\alpha}{\sigma} \right) \right]^{1/2}. \tag{3.3}$$

Again, we can calculate the associated critical delay $\tau_{\text{crit}}^{\text{B}}$,

$$\tau_{\text{crit}}^{\text{B}} = \frac{1}{\omega} \arccos \left(\frac{\omega^2}{\alpha\sigma c} - \frac{1}{c} \right). \tag{3.4}$$

As in Model A, a threshold value $\tau_{\text{crit}}^{\text{B}}$ of the total cooperativity also defines the boundary between stable steady state ($\tau < \tau_{\text{crit}}^{\text{B}}$) and limit cycle ($\tau > \tau_{\text{crit}}^{\text{B}}$). The introduction of another nonlinearity does not change the linear stability analysis performed for Model A. It should be noted, however, that this analysis is an approximation and a more detailed numerical analysis shows that the Hill coefficient threshold is slightly higher than predicted (2.5 instead of 2.0 for fixed $u = 2.0$). The CTD has, as for Model A, a value of CTD $= 53$ min.

Figure 3 shows the stability boundary in (h, τ) space for Models A and B (figure 3a), and the corresponding Hopf period (figure 3b). The region of

oscillatory expression is above and to the right of the (h, τ) curves. For Model B, only the Hill coefficient h is shown. With $u=2$, the total cooperativity coefficient is doubled, leading to almost the same result as for Model B. Thus, for a 120 min period oscillation, the corresponding values of h and τ can be uniquely determined. For Model B, the Hill coefficient required for 120 min period oscillations is greater than 2.5 and the delay smaller than $\max_{h>2.5}(\tau_{\mathrm{crit}}^{\mathrm{B}}) \equiv \tau_{\mathrm{B}} = 20$ min. If an interval between 90 and 150 min for the period is considered, a range for h and τ can be defined as:

— for Model A, $3 < h < 7$ and 15 min $< \tau_{\mathrm{A}} < 30$ min;
— for Model B, $4 < c < 8$, and 10 min $< \tau_{\mathrm{B}} < 30$ min.

These results show that introducing a new mechanism does not affect the basic properties of these models with respect to the Hopf bifurcation. Interestingly, the model considered by Hirata *et al.* (2002) consists of three ODEs with two feedback loops, each with a Hill coefficient of 2 that would give a total cooperativity coefficient of 4. Our comparison of these models reveals general properties of the Hes1 oscillation that are not yet measured experimentally. In particular, strong cooperativity of Hes1 repression (h between 3 and 8) and a turnaround duration between 40 and 60 min are predicted.

(b) *The second nonlinearity increases adaptativity*

The stability results of the previous sections show that oscillation onset of the systems depends on model independent quantities, such as degradation rates, cooperativity coefficients (or the product thereof) and the CTD, including delays due to auxiliary variables. The CTD takes into account both the time-scale introduced by the dynamics of the non-delayed system and the explicit delay τ. However, the behaviour of the solution away from the steady state can be quite different from model to model.

Experimental data on Hes1 expression level in cultured cells after a serum shock show no sign of overshoot in the first cycle of mRNA transcription and Hes1 synthesis (Hirata *et al.* 2002). On the contrary, the expression levels of both mRNA and Hes1 rapidly settle down to an oscillatory regime of approximately constant amplitude. Systems with only one nonlinearity often display a large overshoot before solutions converge to their attractor. A second nonlinearity is then needed to fine-tune the dynamics of the systems when away from equilibrium. In appendix C, using Model A, we compute a lower bound for the value of the Hes1 expression overshoot with respect to the steady-state value.

From the results of a full numerical simulation of Models A and B, we compared the initiation of Hes1 synthesis after a serum shock (figure 4). The serum shock triggers Hes1 transcription and is modelled by setting *Hes1*, *mRNA* and *GroH* initial levels to values close to zero at time 0. In Model A, there is an overshoot due to the lack of repression mechanisms in the first minutes. In the case of Gro/TLE1-mediated repression (Model B), it is assumed that Gro/TLE1 is already active at a low level, and the fast activation rate of Gro/TLE1 supports the rapid convergence of Hes1 expression to the stable oscillatory pattern.

It is possible to give a formal bound for the overshoot. The following calculation shows that the large overshoot (figure 4) is a characteristic feature of
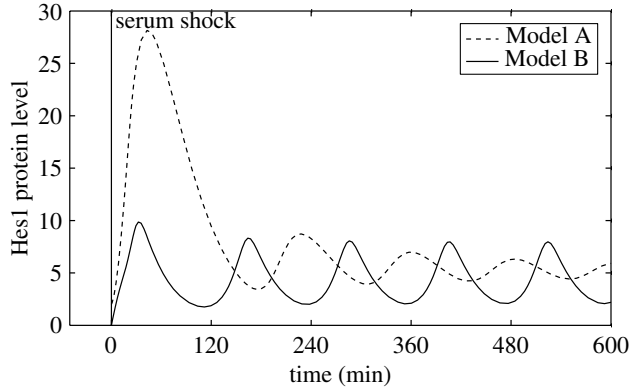
Figure 4. Introduction of a second nonlinearity allows Hes1 protein level to rapidly approach a steady oscillation after initiation by serum shock (solid line), compared with the behaviour of Model A (dashed line).

Model A. We assume that before initiation the *Hes1* gene is practically silent, so the initial conditions for *mRNA* and *Hes*1 are set to zero. Moreover, to simplify the computations, we set $\alpha = \delta$. To obtain a simple expression for the overshoot, we set the transcriptional delay τ equal to the half-lives of Hes1 mRNA and protein, so $\tau = \ln 2/\delta \simeq 23$ min. Calculations of a bound of the overshoot in Hes1 lead to $Hes1_{\mathrm{overshoot}} \geq (1 - \ln 2)\beta f_0/(2\delta^2)$ (see appendix C). With a steady state of $Hes1_* = \beta/\alpha$, the ratio between the maximal protein level and the steady-state level is

$$\frac{Hes1_{\mathrm{overshoot}}}{Hes1_*} = (1 - \ln 2)\frac{f_0}{2\delta}. \tag{3.5}$$

The ratio of maximal transcription to degradation rates, f_0/δ, is large. For instance, $f_0/\delta = 30$ gives an overshoot about five times the steady-state value. It is likely that the ratio f_0/δ is even higher since estimates of 11 initiations per second have been reported (Bolouri & Davidson 2003). It is possible to reduce the overshoot considerably by setting some parameters to unrealistic values. For example, a translation rate β of one translation every 33 min $(0.03\ \mathrm{min}^{-1})$ leads to a smaller overshoot, comparable to Model B simulations. It is likely, however, that β is much larger, ranging from 1.0 to 100 min^{-1} (Ghaemmaghami *et al.* 2003; Bolouri & Davidson 2003). Even though β has no effect on the stability properties of these models, initially it is of crucial importance after serum shock.

In principle, one could replace β in Model A by a nonlinear function without having to take Gro/TLE1–Hes1 interactions into consideration. However, the introduction of this nonlinearity is not motivated by any experimental data and would be artificial.

Compared to Model A, Model B shows a more realistic activation curve. This is due to two factors. First, since Gro/TLE1 is a general corepressor, there may exist a baseline level of phosphorylated protein in the cell before initiation of Hes1 synthesis. This would have an attenuating effect on Hes1 transcription. Second, numerical simulations show that in Model B a smaller delay τ is needed to generate 120 min period oscillations due to the introduction of a second nonlinearity. Consequently, the speed of the response after activation is increased.

4. Discussion

Numerical simulations and analytical results from two models of Hes1 self-regulation show interesting model-independent features. Encouragingly, the most important characteristics of the models all lie in the same range. More precisely, to be consistent with the experimental data the cooperativity coefficient associated with Hes1 repression must be higher than 2, and is likely to be around 4. Further, the explicit delay included in the model should range from 10 to 30 min. These results are in agreement with previous studies (Hirata *et al.* 2002; Jensen *et al.* 2003; Monk 2003; Lewis 2003). Given the complex nature of transcription regulation, it is likely that this parameter plays an important role in the control of protein expression.

A central quantity introduced in this study is the CTD, defined as the CTS + the delay, as a measure of the lag between transcription initiation and repression. In both model versions, a CTD of about 40–60 min is predicted. The model-independent estimation of CTD $\simeq$ 50 min is a central result based only on partial knowledge of kinetic data. A sufficiently large delay is needed to induce oscillations, so the CTS needs to be small. Since the CTS is $2/(\alpha + \delta)$, only protein and mRNA with short half-lives can display these short oscillation periods.

Using linear stability analysis, we estimated the values of the cooperativity coefficients and delays from measured kinetic data, such as Hes1 protein and mRNA degradation rates. Constrained by the period of oscillation, it is possible to define a lower bound for the cooperativity coefficient and an upper bound for the delay. For example, a cooperativity coefficient lower than 4 or a delay longer than 20 min always yield periods longer than 120 min. If the system is near the Hopf bifurcation, these values should be good estimates.

Interaction of Hes1 with Gro/TLE1 is necessary for transcriptional repression by Hes1 (McLarren *et al.* 2001). The fact that Hes1 itself activates hyperphosphorylation of Gro/TLEs suggests a dynamic link between the two proteins. Introduction of Gro/TLE-mediated repression in a model allows a faster physiological adaptation after a serum shock and/or Hes1 induction from the Notch pathway. In feedback loop systems with a single nonlinearity, a large overshoot is seen after initiation, resulting in an initial strong response followed by small amplitude oscillations. When the corepressor Gro/TLE1 is introduced, the overshoot is greatly reduced, and steady oscillatory protein expression levels are observed. Gro/TLE1 is known to be expressed in a variety of cell lines and acts as a general corepressor (Jimenez *et al.* 1997). We suggest that the kinetic role of Gro/TLE1 is to fine-tune expression levels after initiation of protein synthesis.

Editors' note

Please see also related communications in this focussed issue by Benson *et al.* (2006) and Terashima *et al.* (2006).
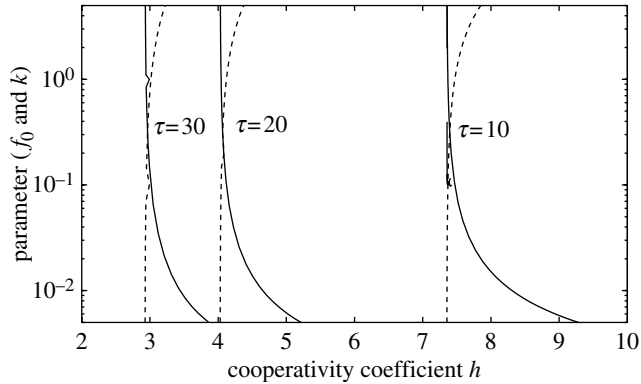
Figure 5. Robustness of the bifurcation parameter h with respect to parameters f_0 (solid lines) and k (dashed lines). Different curves are shown for different values of the delay ($\tau = 10, 20$ and 30 min). Each curve represents the value of either parameter (f_0 or k) at which a Hopf bifurcation occurs when the parameter h is varied. The stability region lies on the left-hand side of the curves.

Appendix A. Linear stability analysis

In this section, we present a detailed linear stability analysis for Model A. The linear analysis for Model B follows the same scheme.

Equations (2.1) and (2.2) are nonlinear differential delay equations with negative feedback. (For a general introduction to delay differential equations and their applications, see Hale & Verduyn-Lunel (1993) and Beuter *et al.* (2003).) The first step of the linear stability analysis is the calculation of the steady states. The equations defining the steady state are

$$\delta mRNA_* = \frac{f_0 k^h}{k^h + Hes1_*^h},$$ (A 1)

$$\alpha Hes1_* = \beta mRNA_*.$$ (A 2)

We note that f_0 and k have only a minor effect on the bifurcation analysis. Even changes of one order of magnitude do not substantially affect the bifurcation analysis (figure 5). For example, a change of k from 0.01 to 1 leads to a change of the bifurcation parameter h from 4.0 to 4.1, at a delay of $\tau = 20$ min. As long as k takes small values, the parameter k can be freely chosen without perturbing the bifurcation analysis of Model A. An appropriate scaling is

$$\left(\frac{k\alpha}{\beta}\right)^h = \frac{\delta}{f_0 - \delta}.$$ (A 3)

With this scaling, the steady-state values are $mRNA_* = 1$ and $Hes1_* = \beta/\alpha$. This is a reasonable assumption since $f_0 \gg \delta$ (see table 1), at least for larger h, as shown in figure 6. There is an excellent agreement between the theoretical bifurcation analysis using the choice of k discussed earlier and numerical bifurcation analysis (figure 6).

Linearization of equations (2.1) and (2.2) around this steady state yields the following equations for the deviations from the steady states $x = mRNA - 1$ and
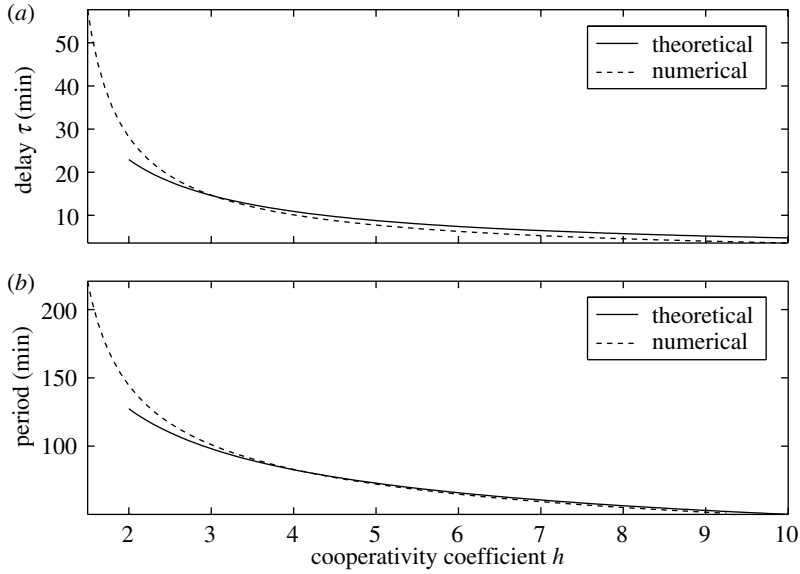
Figure 6. Comparison between theoretical and numerical bifurcation analysis of Model A. (*a*) The numerically computed bifurcation curve (dashed line) shows the value τ at which a Hopf bifurcation occurs when h is varied. The theoretical bifurcation curve (solid line) was drawn using equation (3.4). (*b*) The corresponding period of oscillation (T_{Hopf}) is shown. The numerically computed period (dashed line) is compared to the theoretically computed period (solid line) using $T_{\mathrm{Hopf}} = 2\pi/\omega$ with ω defined in equation (A 11).

$y = Hes1 - \beta/\alpha$:

$$\frac{\mathrm{d}x}{\mathrm{d}t} = -\delta x + f'_* y_\tau, \tag{A 4}$$

$$\frac{\mathrm{d}y}{\mathrm{d}t} = \beta x - \alpha y. \tag{A 5}$$

Here f is the nonlinear function on the right-hand side of equation (2.1) defined by

$$f = f_0 \frac{k^h}{k^h + Hes1^h}. \tag{A 6}$$

Its derivative, evaluated at the steady state f'_*, is given by

$$f'_* = -\frac{\alpha\delta h}{\beta}\left(1 - \frac{\delta}{f_0}\right). \tag{A 7}$$

The characteristic (eigenvalue) equation associated with this system of equations depends on the delay τ,

$$(\lambda + \delta)(\lambda + \alpha) + \alpha\delta h\left(1 - \frac{\delta}{f_0}\right)\exp(-\lambda\tau) = 0. \tag{A 8}$$

There is a critical value for the delay τ, denoted by $\tau_{\mathrm{crit}}^{\mathrm{A}}$, at which the system is destabilized and undergoes a Hopf bifurcation. At this Hopf bifurcation point, a pair of eigenvalues λ has a zero real part, i.e. $\lambda = \pm i\omega$. The value ω gives the

frequency of oscillation at the Hopf bifurcation point. In Model A, the frequency is given by

$$\omega = \frac{1}{\sqrt{2}}\left[-(\delta^2 + \alpha^2) + \left[(\delta^2 - \alpha^2)^2 + 4\alpha^2\delta^2 h^2\left(1 - \frac{\delta}{f_0}\right)^2\right]^{1/2}\right]^{1/2}. \quad (A\,9)$$

The assumption $f_0 \gg \delta$ allows us to simplify the expression for h^A_{crit} (2.3), which is found by solving equation (A 9) with $\omega = 2\pi/T_{\mathrm{Hopf}}$. The oscillation onset (Hopf bifurcation) is given by a sign change of the real part of λ in the characteristic equation for $\lambda = \pm i\omega$. Then, by solving the characteristic equation of Model A (A 8) for τ, we find the relation given in equation (2.4).

A similar analysis for Model B, with the scaling $k^h = \alpha/(f_0 - \beta)$ and $\ell^u = \sigma/(g_0 - \sigma)$, leads to the characteristic equation,

$$(\lambda + \alpha)(\lambda + \sigma) + \Gamma\exp(-\lambda\tau) = 0, \quad \text{with } \Gamma = \alpha h \sigma u\left(1 - \frac{\alpha}{f_0}\right)\left(1 - \frac{\sigma}{g_0}\right). \quad (A\,10)$$

At the Hopf bifurcation, $\lambda = i\omega$ gives

$$\omega = \frac{1}{\sqrt{2}}[-(\alpha^2 + \sigma^2) + [(\alpha^2 - \sigma^2)^2 + 4\Gamma^2]^{1/2}]^{1/2}. \quad (A\,11)$$

By making the approximation that $\Gamma \simeq hu\alpha\sigma$, equation (3.3) and, subsequently, equation (3.4) are obtained.

Appendix B. Characteristic turnaround duration

When $\tau = 0$, Model A reduces to a system of ODEs with a stable steady state. The linearized equations of Model A become linear ODEs, and the eigenvalues λ are given by equation (A 8) with $\tau = 0$. That is,

$$(\lambda + \delta)(\lambda + \alpha) + \alpha\delta h\left(1 - \frac{\delta}{f_0}\right) = 0. \quad (B\,1)$$

Hence, $\lambda = [-(\alpha + \delta) \pm \sqrt{\Delta}]/2$, with a negative discriminant $\Delta < 0$ when $\delta = \alpha$. Thus, the real part of λ is $-(\alpha + \delta)/2$. The turnaround time $|\lambda|^{-1} + \tau$ gives an estimation of the time required from mRNA synthesis to repression of transcription, i.e. a complete turnaround.

The CTD of Models A and B as a function of the cooperativity coefficient (h for Model A and c for Model B) are very similar and vary very weakly (figure 7). When h varies from 4 to 10, the CTD only decreases from 53 to 44 min.

Appendix C. Overshoot and adaptativity

We discuss here the maximal value that solutions of Model A can achieve for initially vanishing Hes1 mRNA. Numerical simulations show that this maximal value is reached around $t = \tau$. This will restrict our search to the interval $t \in (0, \tau]$ leading to a lower bound of the maximal value of Hes1 concentration.

Since the non-delayed terms are linear, Model A can be solved directly with initial conditions given on the interval $[-\tau, 0]$. Setting the initial conditions to
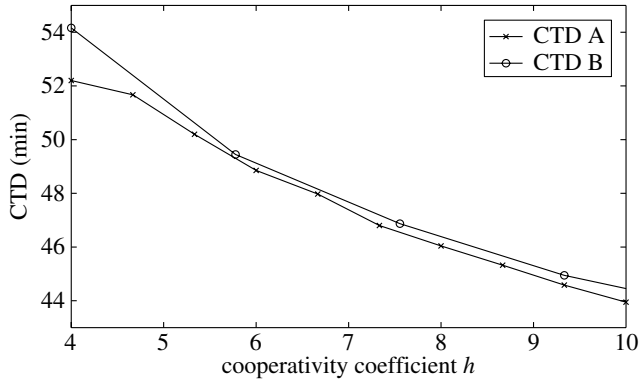
Figure 7. Characteristic turnaround durations for Models A (crosses) and B (open circles). For plotting these curves, a period of 120 min was assumed. That is, for a given h, τ was determined to give a period of 120 min.

zero yields the following system of linear differential equations:

$$\frac{\mathrm{d}mRNA(t)}{\mathrm{d}t} = f_0 - \delta mRNA(t), \tag{C 1}$$

$$\frac{\mathrm{d}Hes1(t)}{\mathrm{d}t} = \beta mRNA(t) - \alpha Hes1(t), \tag{C 2}$$

with the solutions

$$mRNA(t) = \frac{f_0}{\delta}(1 - \mathrm{e}^{-\delta t}), \tag{C 3}$$

$$Hes1(t) = \frac{\beta f_0}{\alpha\delta}\left(1 + \frac{\delta\,\mathrm{e}^{-\alpha t} - \alpha\,\mathrm{e}^{-\delta t}}{\alpha - \delta}\right). \tag{C 4}$$

These solutions are exact for $0 \leq t \leq \tau$ for zero initial conditions. The solution for $Hes1$ is a not a convenient expression, but by letting $\alpha \to \delta$, and evaluating at $t = \tau$, we have

$$Hes1(\tau) = \frac{\beta f_0}{\delta^2}(1 - \mathrm{e}^{-\delta\tau}(1 + \tau\delta)). \tag{C 5}$$

The term in parentheses is a constant of the order of 1. Because estimated values for τ are of the same order as the Hes1 protein and mRNA half-lives, we take the delay τ to be equal to the mRNA half-life, $\tau = \ln 2/\delta$, and we obtain

$$Hes1(\tau) = \frac{\beta f_0}{2\delta^2}(1 - \ln 2). \tag{C 6}$$

If we assume that the steady-state Hes1 level is $Hes1_* = \beta/\alpha = \beta/\delta$, the ratio between $Hes1(\tau)$ and the steady-state Hes1 level can be computed as given in equation (3.5).

References

Benson, A. P., Clayton, R. H., Holden, A. V., Kharche, S. & Tong, W. C. 2006 Endogenous driving and synchronization in cardiac and uterine virtual tissues: bifurcations and local coupling. *Phil. Trans. R. Soc. A* **364**, 1313–1327. (doi:10.1098/rsta.2006.1772)

Beuter, A., Glass, L., Mackey, M. C. & Titcombe, M. S. (eds) 2003. *Nonlinear dynamics in physiology and medicine. Interdisciplinary applied mathematics*, vol. 25. New York: Springer.

Bolouri, H. & Davidson, E. H. 2003 Transcriptional regulatory cascades in development: initial rates, not steady state, determine network kinetics. *Proc. Natl Acad. Sci. USA* **100**, 9371–9376. (doi:10.1073/pnas.1533293100)

Christ, B. & Ordahl, C. P. 1995 Early stage of chick somite development. *Anat. Embryo. (Berl.)* **191**, 381–396. (doi:10.1007/BF00304424)

Ferrell, J. E. J. 1996 Tripping the switch fantastic: how a protein kinase can convert graded inputs into switch-like outputs. *Trends Biochem. Sci.* **21**, 460–466. (doi:10.1016/S0968-0004(96)20026-X)

Gao, X., Chandra, T., Gratton, M. O., Quelo, I., Prud'homme, J., Stifani, S. & St-Arnaud, R. 2001 Hes6 acts as a transcriptional repressor in myoblasts and can induce the myogenic differentiation program. *J. Cell Biol.* **154**, 1161–1171. (doi:10.1083/jcb.200104058)

Ghaemmaghami, S., Huh, W.-K., Bower, K., Howson, R. W., Belle, A., Dephoure, N., O'Shea, E. K. & Weissman, J. S. 2003 Global analysis of protein expression in yeast. *Nature* **425**, 737–741. (doi:10.1038/nature02046)

Goodwin, B. C. 1965 Oscillatory behavior in enzymatic control processes. *Adv. Enzyme Regul.* **3**, 425–438. (doi:10.1016/0065-2571(65)90067-1)

Griffith, J. S. 1968 Mathematics of cellular control processes. I. Negative feedback to one gene. *J. Theor. Biol.* **20**, 202–208. (doi:10.1016/0022-5193(68)90189-6)

Hale, J. K. & Verduyn-Lunel, S. M. 1993 *Introduction to functional differential equations. Applied mathematical sciences*, vol. 99. New York: Springer.

Hirata, H., Yoshiura, S., Ohtsuka, T., Bessho, Y., Harada, T., Yoshikawa, K. & Kageyama, R. 2002 Oscillatory expression of the bHLH factor Hes1 regulated by a negative feedback loop. *Science* **298**, 840–843. (doi:10.1126/science.1074560)

Hoffmann, A., Levchenko, A., Scott, M. L. & Baltimore, D. 2002 The Ikappa B-NF-kappa B signaling module: temporal control and selective gene activation. *Science* **298**, 1241–1245. (doi:10.1126/science.1071914)

Ishibashi, M., Ang, S. L., Shiota, K., Nakanishi, S., Kageyama, R. & Guillemot, F. 1995 Targeted disruption of mammalian hairy and enhancer of split homolog-1 (hes-1) leads to up-regulation of neural helix-loop-helix factors, premature neurogenesis, and severe neural tube defects. *Genes Dev.* **24**, 3136–3148.

Jensen, M. H., Sneppen, K. & Tiana, G. 2003 Sustained oscillations and time delays in gene expression of protein Hes1. *FEBS Lett.* **541**, 176–177. (doi:10.1016/S0014-5793(03)00279-5)

Jimenez, G., Paroush, Z. & Ish-Horowicz, D. 1997 Groucho acts as a corepressor for a subset of negative regulators, including hairy and engrailed. *Genes Dev.* **15**, 3072–3082.

Lev Bar-Or, R., Maya, R., Segel, L. A., Alon, U., Levine, A. J. & Oren, M. 2000 Generation of oscillations by the p53-Mdm2 feedback loop: a theoretical and experimental study. *Proc. Natl Acad. Sci. USA* **97**, 11 250–11 255. (doi:10.1073/pnas.210171597)

Lewis, J. 2003 Autoinhibition with transcriptional delay: a simple mechanism for the zebrafish somitogenesis oscillator. *Curr. Biol.* **13**, 1398–1408. (doi:10.1016/S0960-9822(03)00534-7)

McLarren, K. W., Thériault, F. M. & Stifani, S. 2001 Association with the nuclear matrix and interaction with Groucho and RUNX proteins regulate the transcription repression activity of the basic helix loop helix factor Hes1. *J. Biol. Chem.* **276**, 1578–1584. (doi:10.1074/jbc.M007629200)

Monk, N. A. M. 2003 Oscillatory expression of Hes1, p53, and NF-κB driven by transcriptional time delays. *Curr. Biol.* **13**, 1409–1413. (doi:10.1016/S0960-9822(03)00494-9)

Murray, J. D. 1993 *Mathematical biology. Biomathematics texts*, vol. 19, 2nd edn. Berlin: Springer.

Nuthall, H. N., Husain, J., McLarren, K. W. & Stifani, S. 2002 Role for Hes1-induced phosphorylation in groucho-mediated transcriptional repression. *Mol. Cell. Biol.* **22**, 389–399. (doi:10.1128/MCB.22.2.389-399.2002)

Ohsako, S., Hyer, J., Panganiban, G., Oliver, I. & Caudy, M. 1994 Hairy function as a DNA-binding helix-loop-helix repressor of Drosophila sensory organ formation. *Genes Dev.* **8**, 2743–2755.

Proush, Z., Finley, R. L. J., Kidd, T., Wainwright, S. M., Ingham, P. W., Brent, R. & Ish-Horowicz, D. 1994 Groucho is required for drosophila neurogenesis, segmentation, and sex determination and interacts directly with hairy-related bHLH proteins. *Cell* **79**, 805–815. (doi:10.1016/0092-8674(94)90070-1)

Schnell, S., Maini, P. K., McInerney, D., Gavaghan, D. J. & Houston, P. 2002 Models for pattern formation in somitogenesis: a marriage of cellular and molecular biology. *C. R. Biol.* **325**, 179–189.

Strogatz, S. H. 1994 *Nonlinear dynamics and chaos: with applications to physics, biology, chemistry, and engineering. Studies in nonlinearity.* Reading, MA: Perseus Books.

Terashima, K., Takeuchi, A., Sarai, N., Matsuoka, S., Shim, E. B., Leem, C. H. & Noma, A. 2006 Modelling Cl- homeostasis and volume regulation of the cardiac cell. *Phil. Trans. R. Soc. A* **364**. (doi:10.1098/rsta.2006.1782)

Tyson, J. J. & Othmer, H. G. 1978 The dynamics of feedback control circuits in biochemical pathways. *Prog. Theor. Biol.* **5**, 1–62.